Absorption and Adsorption of Hydrophobic Organic Contaminants to Diesel and Hexane Soot

ARTICLE *in* ENVIRONMENTAL SCIENCE AND TECHNOLOGY · JUNE 2006

Impact Factor: 5.33 · DOI: 10.1021/es052121a · Source: PubMed

2 AUTHORS:

Thanh H Nguyen
University of Illinois, Urbana-Champaign
58 PUBLICATIONS **1,575** CITATIONS
SEE PROFILE

William P Ball
Johns Hopkins University
133 PUBLICATIONS **4,470** CITATIONS
SEE PROFILE

Environ. Sci. Technol. **2006**, *40,* 2958−2964

Absorption and Adsorption of Hydrophobic Organic Contaminants to Diesel and Hexane Soot

THANH H. NGUYEN*,† AND WILLIAM P. BALL

Department of Geography and Environmental Engineering, Johns Hopkins University, 3400 North Charles Street, Baltimore, Maryland 21218

Soot particles vary in pore structure, surface properties, and content of authigenic (native) extractable organic chemicals. To better understand the effects of these properties on sorption, aqueous sorption isotherms for ^{14}C-labeled phenanthrene and 1,2,4-trichlorobenzene were obtained for four soots of varying properties: two diesel reference soots, a hexane soot, and an ozonated hexane soot. Substantial isotherm nonlinearity was observed. In comparison to diesel soot SRM 2975, diesel soot SRM 1650b had a much higher content of extractable authigenic organic chemicals, showed less sorption of ^{14}C-labeled sorbate at low relative concentrations (C_e/S_w), and showed higher sorption at high C_e/S_w. In comparison to normal hexane soot, the ozonated hexane soot had a higher surface O/C ratio and showed substantially less sorption at all concentrations studied. The sorption differences were attributed to the noted differences in properties, and results were interpreted through a dual-mode sorption model that included the possibility of both surface adsorption (modeled using a Polanyi-based approach) and simple phase partitioning (linear absorption). Generally, such modeling indicated that overall uptake at low concentrations in all four soots was dominated by surface adsorption but that sorption at higher sorbate concentrations in SRM 1650b was heavily influenced by linear absorption within the natively bound organic phase.

Introduction

Black carbon (BC) materials are important as sorbents in soils and sediments, and adsorption to these phases has been proposed as a principle cause of sorption nonlinearity for nonpolar hydrophobic chemicals (HOCs), owing to strong adsorption at low sorbate concentration (*1*−*3*). Studies on sorption mechanisms of nonionic organic chemicals by BC have focused on the presumed BC fractions in sediments (*2*, *4*, *5*), residues of biomass burning (*6*−*8*), lampblack (*9*), and some kinds of soot samples (*10*−*13*). These studies found that, at low sorbate concentrations, sorption to environmental BC is roughly between 0.5 and 2 orders of magnitude higher than sorption to typical soil/sediment organic matter. An adsorption process has been proposed in which sorption energetics are controlled by both pore morphology and the chemical nature of sorbate−sorbent interactions (*4*, *5*, *10*, *14*). In addition, oily or tarlike phases can exist as bulk organic phases within soot aggregates (*9*, *13*), and these phases can serve as absorption domains for freshly added chemicals (*9*, *13*).

Unlike activated carbon and some other forms of BC, environmental BC often contains a substantial quantity of authigenic (native) extractable organic chemicals, such as polycyclic aromatic hydrocarbons (PAHs). If present in sufficient quantity, such chemicals may occur as part of a bulk liquid or solid organic phase (*9*, *11*, *15*). It is therefore reasonable to assume that sorption of newly added (e.g., ^{14}C-labeled) chemicals may occur in part through absorption into such native phases. For example, Hong et al. (*9*) used desorption data obtained with five lampblacks to suggest that adsorption was dominant only for PAH sorption by the two lampblacks that had low levels of native organic phase. For the other three lampblacks, the authors suggested that native organic chemicals completely covered the BC surface as a free oily or tarlike phase, into which absorption occurred. The existence of this phase was proven subsequently through microscopic evidence (*16*). Nguyen et al. (*13*) used sorption isotherm data of added ^{14}C-labeled phenanthrene and 1,2,4-trichlorobenzene (TCB) to SRM 2975 to show that adsorption is the dominant mechanism for this particular diesel soot. Jonker et al. (*10*) showed that the distribution coefficients for native PAHs are substantially higher than those for added PAHs. Although these data suggest that at least some of the native PAHs were very slow to desorb (and possibly even trapped inside the soot matrix), they also show that at least some fraction of the native PAHs were accessible to the aqueous phase. The current study extends the work of Nguyen et al. (*13*) by quantifying the adsorption and absorption components of sorption to four reference soots and considering these results in combination with other independently measured soot properties. The four sorbents can be categorized into pairs: (1) a pair of diesel soots that have similar surface O/C ratios but different amount of extractable organic phases and (2) a hexane soot and its ozonated product. The two hexane soots have similar pore size distribution, BET surface area, and amounts of native organic phase, but they differ in their surface O/C ratio. Two of the four soots evaluated (SRM 2975 and SRM 1650b) are samples of emissions from functioning diesel engines (*17*, *18*), and these are intended by the National Institute of Standard and Technology (NIST) to be representative of soot particles. Such particles have been estimated to contribute 77% of anthropogenic $PM_{2.5}$ emissions (*19*). Sorption data for all materials were modeled using both a Freundlich isotherm and a dual-domain model that includes the possibility of separate contributions from linear absorption to the extractable organic phase and nonlinear adsorption to the soot surfaces, as accounted through Polanyi-based modeling. The linear contribution was considered as a necessary modeling component only if a soot's maximum sorption was found to exceed that which could be readily explained on the basis of available surface area and simple adsorption modeling.

Experimental Section

Chemicals and Reagents. ^{14}C-labeled phenanthrene (PHEN) and 1,2,4-trichlorobenzene (TCB) and nonlabeled TCB were obtained from Sigma-Aldrich (Saint Louis, MO). Nonlabeled PHEN in methanol (5 μg/μL) was obtained from Ultra Scientific (North Kingstwon, RI). Specific activities of ^{14}C-labeled PHEN and TCB were 8.2 and 3.3 mCi/mmol, respectively. For batch sorption experiments, the single-

* Corresponding author phone: (203)432-4333; fax: (203)432-2895; e-mail: thn@jhu.edu.

† Current address: Yale University, Department of Chemical Engineering, Environmental Engineering Program, 9 Hillhouse Avenue, New Haven, CT 06511.

10.1021/es052121a CCC: $33.50
Published on Web 03/23/2006

solute spiking solutions contained mixtures of ^{14}C-labeled and nonlabeled chemicals in HPLC-grade methanol (Fisher Scientific).

Sorbents. The four sorbents included a standard reference material of diesel particulate matter from an industrial forklift (SRM 2975), a second standard reference material of diesel engine particulate matter (SRM 1650b), a standard reference hexane soot (*20*), and the same hexane soot after ozonation (oxidized hexane soot). SRM 2975 and SRM 1650b were supplied by NIST (Gaithersburg, MD). The hexane soot and oxidized hexane soot were provided by Dr. D. M. Smith (University of Denver) and were produced using methods described elsewhere (*21*, *22*). For ease of study in batch sorption vessels, the soot materials were immobilized in silica particles, which were purchased as Chromosorb W-AW (catalog no. 23471) from Alltech Associates, Inc. (Deerfield, IL). The immobilization method has been documented by Nguyen et al. (*23*).

Surface O/C ratios were obtained by X-ray photoelectron spectroscopy (XPS), using methods reported by Nguyen et al. (*24*). Results were 0.20, 0.18, 0.10, and 0.20 for the SRM 2975, SRM 1650b, hexane soot, and oxidized hexane soots, respectively. The amounts of extractable native organic phase for SRM 2975 and SRM 1650b are 2% and 20%, respectively, as reported on NIST certificates (*17*, *18*). For the hexane soot, the amount of the extractable phase was found to be 2% by investigators at NIST laboratories, using the same method previously used for SRM 2975 and SRM 1650a. The summed amount of identifiable and quantifiable polycyclic aromatic hydrocarbons (PAHs) for SRM 2975 and SRM 1650b were 120 and 780 μg/g, respectively. Although limited sample supply prevented determination of extractable organic phase for oxidized hexane soot, the amount of quantified PAHs for oxidized hexane soot were similar to those of hexane soot—1200 and 1000 μg/g, respectively. On this basis, we surmise that the amount of total extractable organic phase is likely to also be of similar magnitude, i.e., on the order of 2%.

Methods for BET Specific Surface Area and Pore Size Distribution of Soots and Chars. Nitrogen adsorption data at 77 K were obtained on three soots using a high-resolution gas adsorption analyzer with high-vacuum capacity (3.8×10^{-9} mm of Hg) (ASAP 2010, Micromeritics, Norcross, GA). These data were not collected for oxidized hexane soot, owing to limited sample availability. BET SSA for oxide hexane soot (82 m^2/g) has already been reported in ref 24. For these analyses, approximately 0.1 g of soot was used. Because we are most interested in properties of the untreated ("as-received") materials on which sorption experiments were conducted, two pretreatment procedures were applied to investigate the effects of the outgassing pretreatment on surface area and pore volume measurements from N_2 adsorption data. For a first set of samples, the sample tubes were outgassed under high vacuum (3.8×10^{-9} mm of Hg) at 300 °C for 5 h prior to analysis, in accordance with the American Society for Testing and Materials Standards for powdered BC samples (*25*). Subsequently, sample tubes were removed from the outgassing port and weighed to determine the outgassed sample mass. Following recommendations of the instrument manufacturer (*26*), samples were then heated for an additional period of 1 h at 250 °C under high vacuum at the analyzing port to ensure complete removal of any physically entrapped gas. Without this step, some samples continued to outgas during initial slow equilibration at ultrahigh vacuum. High-resolution multipoint nitrogen adsorption data were then collected at 77 K in the range of 10^{-7} to 0.995 relative pressure (P/P_o, where P_o is approximately 780 mm of Hg for N_2 at 77 K). Incremental dosing with the dose amount set at 0.3 mL/g was used between 10^{-7} to 10^{-2} P/P_o (i.e., a data point was collected each time the sample had adsorbed 0.3 mL of N_2 per gram of sample). In the range of 10^{-2} to 0.995 P/P_o, data points were collected according to a pressure table containing a list of preset pressures. For a second set of soot samples, outgassing was conducted at room temperature to minimize the removal of natively bound semivolatile organic phases. Specifically, samples were outgassed under high vacuum for 24 h on the outgassing port and another 24 h on the analysis port before final analysis (both at room temperature) and then analyzed as with the first set. The first set will be referred to hereafter as "heated samples" and the second set as "unheated samples".

All collected data (between 70 and 95 points) were modeled for pore size distribution using both (1) nonlocal DFT and an assumption of slitlike pores (*27*) and (2) the BJH model that assumes cylindrical pores (*28*). Data in the range of 0.06−0.2 P/P_o were modeled separately using the conventional BET technique for specific surface area estimation (BET-SSA) (*29*).

Sorption Experiments. Flame-sealed glass ampules with nominal sizes of 10 mL and 5 mL were used for bottle-point batch sorption experiments with PHEN and TCB, respectively. Details on prewetting of sorbents, solute spiking, and sorbent−liquid separation can be found in ref *23*. Briefly, soot−silica mixtures were used as sorbents with all sorption attributed to the soot phase. An equilibration time of 60 days was used for all samples, with final solid/liquid separation achieved by centrifugation at 2056*g* for 1 h. A volume of 1 mL of supernatant was withdrawn and injected into scintillation vials for 10 min counting (model LS3801, Beckman Instrument, Fullerton, CA). Between three and five replicates were conducted at each concentration, and three replicate blank samples (without sorbent) were included at each concentration. Losses were confirmed to be minor (<5%) and proportional to aqueous concentration. Sorbed concentrations in nonblank samples were then determined by difference from aqueous measurements after correction for losses (*30*).

Isotherm model regressions were performed using commercial software (Sigma Plot 2000, SPSS, Chicago, IL), which uses the Marquart−Levenberg algorithm to estimate unknown model parameters by minimizing the squared error on the dependent variable (sorbed concentration). The isotherm models used were the solubility-normalized Freundlich eq 1a (*1*, *31*) and an adaptation of the Polanyi−Manes adsorption model (eq 1b; (*1*)) that follows the Dubinin−Astakhov form (*32*).

$$q_e = K_f^*(C_e/S_w)^n \tag{1a}$$

$$q_e = (q'_{ad,max}\rho_{sorbate})\ \exp\left[-c\left[\frac{RT\ln(S_w/C_e)}{N}\right]^d\right] \tag{1b}$$

In eq 1a, C_e and q_e are the aqueous and adsorbed concentrations at equilibrium, respectively (e.g., in units of μg/mL and μg/g), n is an empirical exponent (typically less than 1), and K_f^* (μg/g) is the modified Freundlich coefficient. In eq 1b, $q'_{ad,max}$ is the maximum adsorption capacity in units of sorbate volume (μL sorbate/g sorbent), $\rho_{sorbate}$ is the assumed sorbate density (μg/μL, based on neat chemical density at the sorption temperature), and $\epsilon_{sw} = RT\ln(S_w/C_e)$ is the adsorption potential (J/mol). For weakly polar sorbates adsorbing on BC surfaces, the normalizing factor N can be usefully equated to V_s (molar volume, mL/mol) and the quantity $RT\ln(S_w/C_e)/V_s$ reported as adsorption potential density (*33*−*35*). This leaves $q'_{ad,max}$, c, and d as fitting parameters for the isotherm.

Results and Discussion

BET Specific Surface Area and Pore Size Distribution of Soots. Figure 1S (Supporting Information) shows that

TABLE 1. DFT and BJH Pore Size Distributions and BET-SSA for Studied Samples

		DFT model results					BJH model results			
samples	BET-SSA (m^2/g)	pore width <10 Å[a]	pore width 10−20 Å[a]	pore width 20−500 Å[a]	pore width 500−2500 Å[a]	total pore volume[a]	pore width 10−20 Å[a]	pore width 20−500 Å[a]	pore width 500−2000 Å	total pore volume[a]
SRM 2975 (not heated during outgassing)	80	0.0000 (0.0%)	0.0114 (4.4%)	0.1058 (40.4%)	0.1446 (55.2%)	0.2619	0.0 (0.0%)	0.0758 (38.6%)	0.1207 (61.4%)	0.1965
SRM 2975 (heated during outgassing)	87	0.0006 (0.4%)	0.0050 (3.0%)	0.0665 (40.9%)	0.0904 (55.7%)	0.1624	0.0 (0.0%)	0.1350 (53%)	0.1197 (47%)	0.2547
SRM 1650b (not heated during outgassing)	48	0.0000 (0.0%)	0.0012 (0.8%)	0.0682 (47.4%)	0.0746 (51.8%)	0.1440	0.0 (0.0%)	0.0622 (48.9%)	0.0651 (51.1%)	0.1274
SRM 1650b (heated during outgassing)	80	0.0000 (0.0%)	0.0057 (2.4%)	0.1235 (52.7%)	0.1051 (44.9%)	0.2343	0.0 (0.0%)	0.1177 (56.6%)	0.0901 (43.4%)	0.2078
hexane soot (not heated during outgassing)	81	0.0000 (0.0%)	0.0091 (5.7%)	0.0828 (51.3%)	0.0694 (43.0%)	0.1613	0.0 (0.0%)	0.1060 (60.2%)	0.0700 (39.8%)	0.1760
hexane soot (heated during outgassing)	87	0.0011 (0.9%)	0.0094 (7.7%)	0.0562 (45.9%)	0.0555 (45.4%)	0.1222	0.0 (0.0%)	0.1091 (59.2%)	0.0753 (40.8%)	0.1844

[a] Pore volume in mL/g (percentage).

nitrogen adsorption for both heated and unheated samples of SRM 2975, SRM 1650b, and hexane soot increased rapidly with P/P_o for P/P_o up to 0.2, but only gradually up to $P/P_o = 0.9$, and again rapidly up to $P/P_o = 0.99$. According to the IUPAC classification (*36*), these isotherms are classified as type II for nonporous or mesoporous/macroporous materials.

Because all soot contains some native organic chemicals that may volatilize under evacuation but remain with the soot under aqueous conditions, comparison of BET-SSA and pore size distribution should arguably be made on measurements obtained with nonevacuated (as-received) samples. This selection is "arguable" in the sense that it assumes that authigenic PAH will be equally effective at blocking the gas-phase adsorption of N_2 (at low temperature) and aqueous-phase PHEN or TCB (at room temperature). Although this assumption is in contrast to recent findings that NOM can affect BET-SSA of chars without affecting benzene sorption from solution (*14*), authigenic PAHs in soot are likely to be much smaller and less flexible than NOM sorbed in char, and we expect them to enter or block pores and to compete directly with PHEN and TCB for soot adsorption sites. BET-SSA analysis of untreated samples was not possible, however, because of the continuous release of such preadsorbed species that would occur during nitrogen gas adsorption under evacuated conditions. Nonetheless, it is clear that outgassing at 300 °C can remove a substantial quantity of native organic phase, relative to that present in the untreated samples that were used for sorption study. To provide more realistic assessments of relevant pore volumes and surface areas for the soots used in sorption experiments, we also conducted BET-SSA analysis following outgassing at room temperature.

For SRM 2975 and hexane soot, the heated samples adsorbed only slightly more nitrogen than the unheated samples (Figure 1Sa,b). The heated sample of SRM 1650b, however, adsorbed significantly more nitrogen than the unheated sample, with most differences occurring at $P/P_o < 0.9$ (Figure 1Sc). As a result, the difference in BET-SSA for heated and unheated SRM 1650b (80 vs 48 m^2/g) is much higher than the corresponding differences for SRM 2975 (87 vs 80 m^2/g), and heated hexane soot (87 vs 81 m^2/g). For a different batch of similar diesel particulates (SRM 1650), Bucheli and Gustafsson (*12*) reported that a decrease in outgassing temperature from 300 to 100 °C led to a decrease of BET-SSA from 89 to 48 m^2/g. Because SRM 1650b has 10 times more extractable organic phase than SRM 2975 and hexane soot (*17*, *18*), it is reasonable to assume that the presence of native organic phases is the cause for this difference. For the unheated samples, the BET-SSA of SRM 1650b is roughly 60% that of SRM 2975 and hexane soot and also ~60% that in heated samples for all three soots. Similar results were reported in ref *37* for naphthalene-containing sand and silica gel samples and in ref *14* for lipid-containing synthetic chars. For reasons described in the preceding paragraph, the data from unheated samples are believed to be the most appropriate for use in interpreting PHEN and TCB sorption results from aqueous solution on as-received material.

Pore size distribution data for unheated soot samples are shown in Table 1. All three soots have substantial pore volume in size ranges corresponding to mesopores (20−500 Å) and macropores (>500 Å). Because the accuracy of the DFT model decreases with increasing pore width (*38*), however, the pore volume estimates for the macropore range shown in Table 1 are not likely to be accurate. This may explain why the DFT model shows more total pore volume for the unheated soot SRM 2975 and hexane soot than for the heated samples (Table 1).

As with the data obtained by the DFT model, the pore size distributions suggested by the BJH model also show an absence of micropores but substantial volumes in the mesopore range. The BJH model, unlike the DFT model, does indicate higher total pore volume in heated samples, which better follows expectations. The limitation of the BJH model, however, is that it can be applied only to pores with diameters of 10−2000 Å. Nonetheless, the BJH modeling corroborate the DFT finding that these are predominantly mesoporous materials and that preevacuation at high temperature increases the measured mesopore volume.

Freundlich Sorption Isotherm Modeling. Figure 1a−d represents sorption data collected at final (equilibrium) relative concentrations (C_e/S_w) between 3.0×10^{-4} and 0.6 for PHEN and between 2.0×10^{-4} and 0.6 for TCB. To help visualize trends and compare overall isotherm nonlinearity, this figure also contains regression equations for the log-transformed data using the normalized Freundlich model (eq 1a).

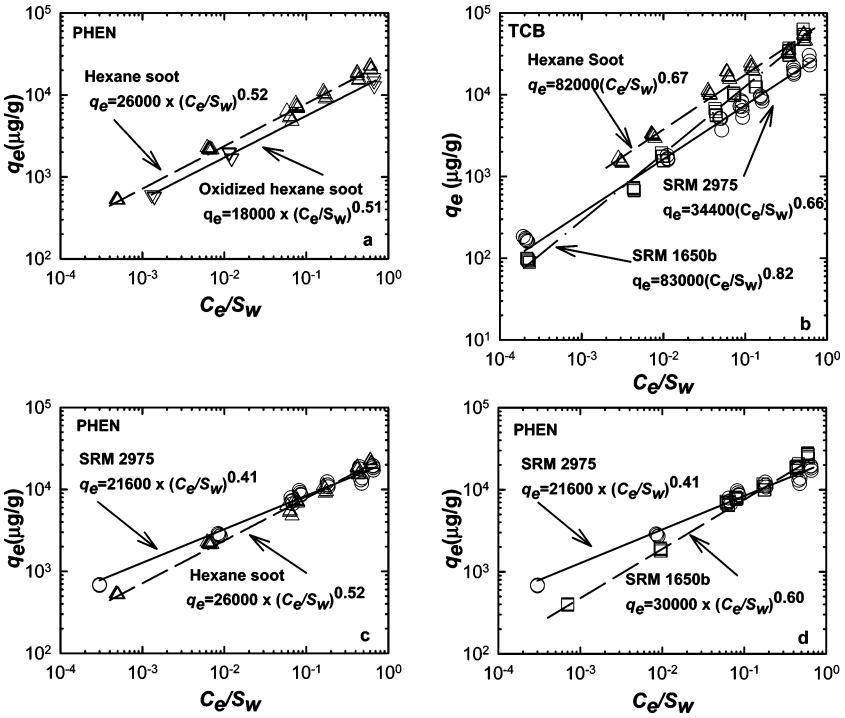

FIGURE 1. Freundlich sorption isotherms of phenanthrene with hexane soot and oxidized hexane soot (a), hexane soot and SRM 2975 (c), SRM 2975 and SRM 1650b (d). Freundlich sorption isotherms of TCB with SRM 2975, SRM 1650b, and hexane soot (b). Isotherm equations are shown in the figure. Details about isotherms and goodness-of-fit for all cases can be found in Table 1S (Supporting Information).

As apparent from Figure 1a, PHEN sorption isotherms for hexane soot and oxidized hexane soot are parallel in the log−log plot, with Freundlich exponents that are statistically the same (0.52 ± 0.01 vs 0.51 ± 0.01). The adsorption affinity (K_f^*) is 150% higher for the normal hexane soot than for oxidized hexane soot. These two soots have similar surface areas and have similar summed concentrations of identified and quantified PAHs (see Sorbents in the Experimental Section); however, they have very different surface chemistry, as indicated by O/C ratios (0.1 for hexane soot vs 0.2 for oxidized hexane soot) (*24*). Because the ozonated soot surfaces contain more oxygen-containing functional groups (*21*), water can more effectively compete for sorption sites, causing sorption of PHEN to the ozonated soot to be less energetically favorable. Observations follow this expectation at all concentrations measured.

Another pair of parallel isotherms on the log−log plot is that of TCB sorption by SRM 2975 and hexane soot (Figure 1b). Again, the Freundlich exponents are statistically the same (n = 0.66 ± 0.03 vs 0.67 ± 0.02). K_f^* is much higher for the hexane soot than for SRM 2975. These observations are also consistent with expectations based on O/C ratios (0.1 for hexane soot vs 0.2 for SRM 2975). Note that these two soots have similar BET-SSA (81 vs 80 m^2/g) and similar percentages of extractable native organic phase (2%). Moreover, the observation that sorption is similarly affected at all studied concentrations, combined with prior evidence for adsorption dominance in SRM 2975 (*13*), suggest that adsorption is the primary sorption mechanism and that TCB adsorption mechanisms are similar for both materials at all concentrations studied. For the case of PHEN sorption isotherms with SRM 2975 and hexane soot are not parallel (Figure 1c). These results reflect different mechanisms and sites of adsorption for PHEN than TCB with at least one of the two soots. More particularly, a comparison of TCB and PHEN isotherms (Figure 1, part b vs part c) shows that hexane soot uniformly sorbs more TCB than PHEN at all C_e/S_w, but that SRM 2975 shows greater TCB sorption only at high C_e/S_w. Thus, SRM 2975 is able to sorb more PHEN than TCB only for high-energy sites. This may be a consequence of the greater planarity of PHEN, which could allow better access to slitlike pores and stronger specific interaction with PAH-like moieties in the SRM 2975 soot (*39*). Apparently, such preferential PHEN interactions at low C_e/S_w are absent from the hexane soot.

Compared to SRM 2975, SRM 1650b showed more linear isotherms for both TCB and PHEN (Figure 1, parts b and d), with correspondingly higher Freundlich exponents (0.60 ± 0.03 vs 0.41 ± 0.02 for PHEN and 0.82 ± 0.03 vs 0.66 ± 0.03 for TCB). Careful examination of these soots' isotherms (Figure 1, parts b and d) shows that the curves cross, with SRM 2975 sorbing more strongly at low C_e/S_w and SRM 1650b sorbing more strongly at high C_e/S_w. The crossover points are ∼0.003 for TCB and ∼0.1 for PHEN. The major difference between these two soots is that SRM 1650b contains 10 times more extractable organic phase than SRM 2975 (20% vs 2%) (*17*, *18*). Note that the two soots have similar O/C ratios (0.20 for SRM 2975 and 0.18 for SRM 1650b) such that the effect of surface hydrophobicity is not likely to be important. We hypothesize that absorption into the native organic phase is significant for the SRM 1650b at high C_e/S_w and causes overall sorption to be greater than that observed for SRM 2975 at these high concentrations. At low concentrations, on the other hand, adsorption dominates and the SRM 2975 has a higher number of available high-energy sites. For SRM 1650b, many such sites are occupied or blocked by native PAHs. Thus, the HOCs associated with this phase may cause both (1) reduced adsorption at low concentrations (because of the lower numbers of available high-energy adsorption sites) and (2) enhanced absorption at the higher concentrations because of partition within some fraction of the native organic phase that occupies some part of the SRM 1650b surface.

Polanyi-Based Sorption Isotherm Modeling. As in our previous work on SRM 2975 (*24*), we fitted sorption results for SRM 2975 and hexane soot using eq 1b to test the hypothesis that adsorption is the dominant sorption mechanism. Excellent fits to data were obtained in all cases (Figure 2a−d), as reflected by mean weighted square error (MWSE) values (Table 2S; Supporting Information).

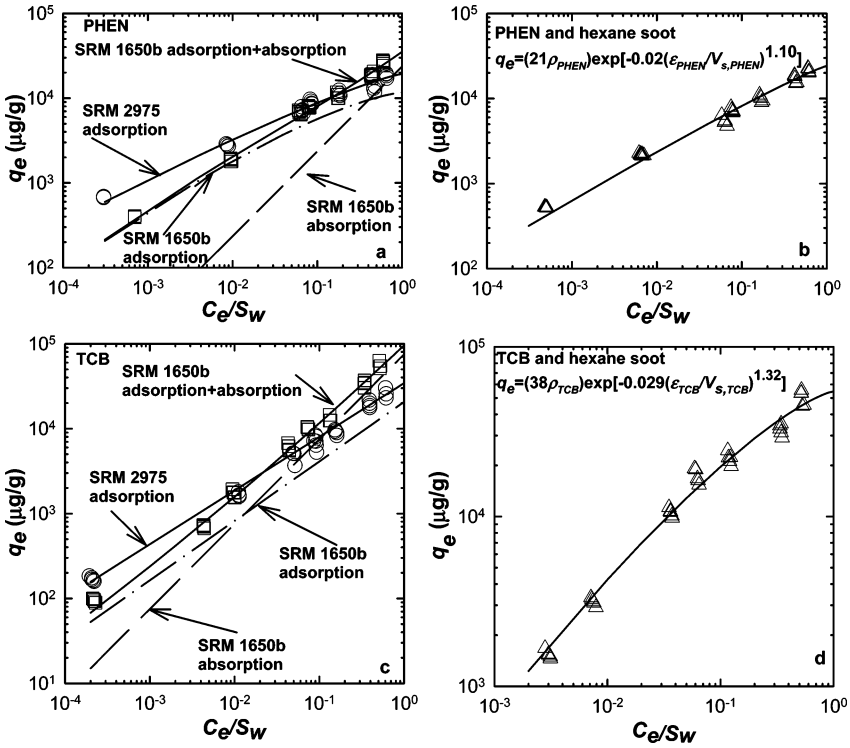

FIGURE 2. Phenanthrene sorption isotherms for SRM 2975 and SRM 1650b (a) and for hexane soot (b). TCB sorption isotherms for SRM 2975 and SRM 1650b (c) and hexane soot (d). Also shown are adsorption and absorption components for SRM 1650b. Isotherm equations for hexane soot are shown in parts b and d. For SRM 2975 and hexane soot, the "absorption" contribution has been assumed negligible. The values of $q'_{ad,max}$ are taken as $C_e/S_w = 1.0$. Isotherm equations for SRM 2975, SRM 1650b, and oxidized hexane soot are as follows: SRM 2975/PHEN $q_{e,PHEN} = (17\rho_{PHEN})\exp[-0.011(\epsilon_{PHEN}/V_{s,PHEN})^{1.18}]$; SRM 2975/TCB $= q_{e,TCB} = (24\rho_{TCB})\exp[-0.03(\epsilon_{TCB}/V_{s,TCB})^{1.00}]$; SRM 1650b/PHEN $q_{e,PHEN} = 91300f_{op}C_e + (10\rho_{PHEN})\exp[-0.005(\epsilon_{PHEN}/V_{s,PHEN})^{1.37}]$; SRM 1650b/TCB $q_{e,TCB} = 11000f_{op}C_e + (14\rho_{TCB})14\exp[-0.036(\epsilon_{TCB}/V_{s,TCB})^{1.00}]$; oxidized hexane soot/PHEN $q_{e,PHEN} = (14\rho_{PHEN})\exp[-0.02(\epsilon_{PHEN}/V_{s,PHEN})^{1.10}]$; the isotherm for oxidized hexane soot with PHEN is not shown in these figures for clarity. Note that no isotherms were collected for TCB with oxidized hexane soot owing to a shortage of this material. Details about isotherms and goodness-of-fit for all cases can be found in Tables 2S and 3S (Supporting Information). Physical and chemical properties of the studied sorbates are listed in Table 4S.

For SRM 2975 and hexane soot, simple adsorption (without absorption contribution) was found adequate to fit the observed isotherms, with $q'_{ad,max}$ values as shown in Figure 2 a−d. The $q'_{ad,max}$ values for both sorbates with both soots are well within the bounds of expectations on the basis of adsorption to measured BET-SSA, even using the lower BET-SSA estimates following nonheated evacuation. Specifically, BET-SSA-normalized sorption capacity ($q'_{ad,max}$/BET-SSA) for SRM 2975 and hexane soot were 0.20 μL/m^2 (0.23 mg/m^2) and 0.25 μL/m^2 (0.29 mg/m^2), respectively, for PHEN, and 0.30 μL/m^2 (0.43 mg/m^2) and 0.46 μL/m^2 (0.67 mg/m^2) for TCB. These values are significantly smaller than that previously observed by others for TCB adsorption to activated carbon F-400 (0.57 μL/m^2 or 0.83 mg/m^2), as calculated from the measured maximum adsorption capacity (0.54 mL/g shown in Figure 3 of ref *40*) and separately measured BET-SSA (948 m^2/g from ref *41*). Moreover, $q'_{ad,max}$/BET-SSA for all three soots at low C_e/S_w were over 10 times lower than those reported for the activated carbons. The comparison suggests that the observed adsorption is certainly reasonable with respect to measured BET-SSA. Note that activated carbons are microporous such that a higher percentage of surface area is associated with pore filling at low C_e/S_w, hence, the 10 times greater sorption at low C_e/S_w.

For SRM 1650b, the reduced isotherm sorption nonlinearity with both sorbates suggests that the overall sorption is the summation of adsorption and absorption domains. Therefore we used the dual-domain model (eq 2).

$$q_e = K_{op}f_{op}C_e + (q'_{ad,max}\rho_{sorbate})\exp\left[-c\left[\frac{RT\ln(S_w/C_e)}{V_s}\right]^d\right] \quad (2)$$

K_{op} is the solute distribution coefficient with the soot organic phase (mL/g) and f_{op} is the fraction of extractable organic phase (i.e., 0.20 for SRM 1650b). This model was previously applied in the context of sorption to SRM 2975 (*13*), but for that material the absorption contribution ($f_{op}K_{op}C_e$) was found to be unimportant to overall sorption. For application of eq 2 to SRM 1650b, we assume that the $q'_{ad,max}$ of SRM 1650b equals 60% of the $q'_{ad,max}$ observed for SRM 2975, based on the previously discussed values of BET-SSA and total pore volumes for heated and unheated SRM 1650b. With $q'_{ad,max}$ thus fixed at 10 μL/g for PHEN and 14 μL/g for TCB, the "most likely" values of c, d, and K_{op} for SRM 1650b were obtained by conducting a nonlinear regression of eq 2 on the sorption data, with results as shown in Table 3S (Supporting Information).

The K_{op} for PHEN from the aforementioned data fitting was then used to estimate an effective average molecular weight MW_{op} for the organic phase. This was done by applying the definition of K_{op} (*39*) with an assumption that phenantherene dissolution in native organic phases follows Raoult's law for ideal solution (i.e., γ_{op} = 1 mol solute/mol op).

$$K_{op} = \frac{1}{\gamma_{op}MW_{op}S} \quad (3)$$

S is the solubility of the subcooled liquid (mol solute/mL water).

A similar fitting exercise for K_{op} was conducted using the sorption isotherm data for TCB with SRM 1650b. With the use of the fitted K_{op} for TCB and the value of MW_{op} found from K_{op} for phenantherene, the activity coefficient (γ_{op}) for TCB was estimated. This approach was taken because TCB dissolution in the native organic phase of soot is probably not ideal. The results are shown in Table 3S (Supporting Information). K_{op} for PHEN with SRM 1650b is estimated at 91 300 mL/g which, with application of eq 3, suggests that MW_{op} = 316 Da (g op/mol op). The estimated MW seems reasonable in light of data from Apicella et al. (*42*), who used size exclusion chromatography to find that the dichloromethane-soluble fraction of a diesel soot had a MW between 200 and 300 Da. The value of logK_{op} for phenantherene is 4.96, which is twice that of the highest reported value in ref *43* for soils and sediments. This too is reasonable, given that soil/sediment organic matter contains various polar and nonpolar organic fractions, while the organic phase in soot is likely to comprise primarily aromatic hydrocarbons.

When MW_{op} = 316 (g op/mol op) and eq 3 are applied using K_{op} = 11 000 mL/g for TCB (Table 3S; Supporting Information), γ_{op} is found equal to 1.52 for TCB dissolution in the organic phase, which is also a reasonable value. For example, Peters et al. (*44*) estimated γ_{op} for different HOCs with four coal tars and reported γ_{op} ranging from 0.14 to 1.27. Only PAH compounds were found to have γ_{op} equal to 1.0 or less. Substituted benzenes (ethylbenzene, xylenes, and styrene) all showed γ_{op} significantly greater than 1.0.

As previously described in the Introduction, Hong et al. (*9*) have suggested that lampblack samples can be divided into two categories. For the first category (including CA-2 and CA-5 of Hong et al.), native PAHs adsorb on the surface of lampblack and occupy adsorption sites. For the second category (including CA-10, CA-17, and CA-18 of Hong et al.), native PAHs occupy the entire adsorption surface as a free oil or tarlike phase. Our results with SRM 2975 and hexane soot suggest that sorption to these soots fall into the first category, with adsorption dominant. On the other hand, SRM 1650b shows mixed behavior, with adsorption dominant at low concentration and absorption contributing at high concentration. This soot therefore belongs to a third category of BC materials, for which a limited number or adsorption sites are available but for which a sufficient volume of organic phase is available (presumably external to pores) for some absorption to occur. The three categories of soot and lampblack samples are schematically illustrated in Figure 2S (Supporting Information).

In summary, the results of this work clearly indicate that the extents of HOC interaction with soot at various sorbate concentrations are strongly dependent on soot characteristics. The experimental evidence indicates that adsorption dominates HOC sorption with three soots (SRM 2975, hexane soot, and oxidized hexane soot) at all studied concentrations of sorbate but that sorption with the fourth soot (SRM 1650b) is best described by a dual-domain model that accounts for significant absorption impact at high relative sorbate concentration. Sorption isotherms were found to be strongly nonlinear for all soots studied, and differences among soots were attributed to different amounts of extractable native organic phase and different surface chemistries. Clearly, the K_{oc} value of any given HOC with environmental BC will depend not only on the HOC concentration but also upon the type of BC being considered. Additional work is needed to better understand the relations between HOC sorption characteristics and BC properties. Nonetheless, this work clearly shows that both adsorption and absorption are important processes with these materials and that surface chemistry and authigenic organic phase content are important parameters to consider.

Acknowledgments

This work was supported by the National Science Foundation under Grant No. BES-0332160. We thank Dr. Dwight Smith (University of Denver) and Dr. Dianne Poster (NIST) for providing the soot samples and Ms. Hee-Kyong Kim and Ms. Supria Ranade (JHU undergraduate students) for assisting with sorption experiments. Dr. Poster in the Analytical Chemistry Division of NIST analyzed all soots for individual PAH concentrations and the hexane soot for total extractable organic matter. Dr. Poster also provided helpful insight into these results and editorial assistance with the manuscript.

Supporting Information Available

Nitrogen isotherm data for SRM 1650b, SRM 2975, and hexane soot samples (Figure 1S); the sorption mechanisms with the various soot and lampblack samples (Figure 2S); fitted parameters of observed sorption data by Freundlich isotherms (Table 1S); fitted parameters of observed sorption data by Polanyi-based isotherms (Table 2S); fitted parameters of observed sorption data by the dual-mode model for SRM 1650b (Table 3S); sorbate physical and chemical properties used for modeling (Table 4S). This material is available free of charge via the Internet at http://pubs.acs.org.

Literature Cited

(1) Allen-King, R. M.; Grathwohl, P.; Ball, W. P. New Modeling Paradigms for the Sorption of Hydrophobic Organic Chemicals to Heterogeneous Carbonaceous Matter in Soils, Sediments, and Rocks. *Adv. Water Res.* **2002**, *25*, 985−1016.

(2) Accardi-Dey, A.; Gschwend, P. M. Assessing the Combined Roles of Natural Organic Matter and Black Carbon as Sorbents in Sediments. *Environ. Sci. Technol.* **2002**, *36* (1), 21−29.

(3) Cornelissen, G.; Gustafsson, O.; Bucheli, T. D.; Jonker, M. T. O.; Koelmans, A. A.; van Noort, P. C. M. Extensive Sorption of Organic Compounds to Black Carbon, Coal, and Kerogen in Sediments and Soils: Mechanisms and Consequences for Distribution, Bioaccumulation, and Biodegradation. *Environ. Sci. Technol.* **2005**, *39* (18), 6881−6895.

(4) Cornelissen, G.; Elmquist, M.; Groth, I.; Gustafsson, O. Effect of Sorbate Planarity on Environmental Black Carbon Sorption. *Environ. Sci. Technol.* **2004**, *38* (13), 3574−3580.

(5) Lohmann, R.; MacFarlane, J. K.; Gschwend, P. M. Importance of Black Carbon to Sorption of Native PAHs, PCBs, and PCDDs in Boston and New York, Harbor Sediments. *Environ. Sci. Technol.* **2005**, *39* (1), 141−148.

(6) Yang, Y. N.; Sheng, G. Y. Enhanced Pesticide Sorption by Soils Containing Particulate Matter from Crop Residue Burns. *Environ. Sci. Technol.* **2003**, *37* (16), 3635−3639.

(7) Braida, W. J.; Pignatello, J. J.; Lu, Y. F.; Ravikovitch, P. I.; Neimark, A. V.; Xing, B. S. Sorption Hysteresis of Benzene in Charcoal Particles. *Environ. Sci. Technol.* **2003**, *37* (2), 409−417.

(8) Sander, M.; Pignatello, J. J. Characterization of Charcoal Adsorption Sites for Aromatic Compounds: Insights Drawn from Single-Solute and Bi-Solute Competitive Experiments. *Environ. Sci. Technol.* **2005**, *39* (6), 1606−1615.

(9) Hong, L.; Ghosh, U.; Mahajan, T.; Zare, R. N.; Luthy, R. G. PAH Sorption Mechanism and Partitioning Behavior in Lampblack-Impacted Soils from Former Oil-Gas Plant Sites. *Environ. Sci. Technol.* **2003**, *37* (16), 3625−3634.

(10) Jonker, M. T. O.; Koelmans, A. A. Sorption of Polycyclic Aromatic Hydrocarbons and Polychlorinated Biphenyls to Soot and Soot-Like Materials in the Aqueous Environment: Mechanistic Considerations. *Environ. Sci. Technol.* **2002**, *36* (17), 3725−3734.

(11) Jonker, M. T. O.; Koelmans, A. A. Extraction of Polycyclic Aromatic Hydrocarbons from Soot and Sediment: Solvent Evaluation and Implications for Sorption Mechanism. *Environ. Sci. Technol.* **2002**, *36* (19), 4107−4113.

(12) Bucheli, T. D.; Gustafsson, O. Quantification of the Soot-Water Distribution Coefficient of PAHs Provides Mechanistic Basis for Enhanced Sorption Observations. *Environ. Sci. Technol.* **2000**, *34* (24), 5144−5151.

(13) Nguyen, T. H.; Sabbah, I.; Ball, W. P. Sorption Nonlinearity for Organic Contaminants with Diesel Soot: Method Development and Isotherm Interpretation. *Environ. Sci. Technol.* **2004**, *38* (13), 3595−3603.
(14) Kwon, S.; Pignatello, J. J. Effect of Natural Organic Substances on the Surface and Adsorptive Properties of Environmental Black Carbon (Char): Pseudo Pore Blockage by Model Lipid Components and Its Implications for N-2-Probed Surface Properties of Natural Sorbents. *Environ. Sci. Technol.* **2005**, *39* (20), 7932−7939.
(15) Poster, D. L.; Lopez de Alda, M. J.; Schantz, M. M.; Sander, L. C.; Wise, S. A.; Vangel, M. G. Development and Analysis of Three Diesel Particulate-Related Standard Reference Materials for the Determination of Chemical, Physical, and Biological Characteristics. *Polycyclic Aromat. Compd.* **2003**, *23* (2), 141−191.
(16) Hong, L. Sorption of Polycyclic Aromatic Hydrocarbons to Lampblack and Polyoxymethylene. Civil and Environmental Engineering, Ph.D. Dissertation, Stanford University, 2006.
(17) National Institute of Standards and Technology. *Certificate of Analysis—Standard Reference Material 2975—Diesel Particulate Matter (Industrial Forklift)*; National Institute of Standards and Technology: Gaithersburg, MD, 2001.
(18) National Institute of Standards and Technology. *Certificate of Analysis—Standard Reference Material 1650a—Diesel Particulate Matter*; National Institute of Standards and Technology: Gaithersburg, MD, 2001.
(19) *Health Assessment Document for Diesel Engine Exhaust*, Report; USEPA National Center for Environmental Assessment; Washington, DC, 2002.
(20) Schmidt, M. W. I.; Massiello, C. A.; Skjemstad, J. O. Final recommendations for reference materials in black carbon analysis. *Eos*, *Transactions*, *Amer. Geophys. Union* **2003**, *84* (12), 582−583.
(21) Chughtai, A. R.; Williams, G. R.; Atteya, M. M. O.; Miller, N. J.; Smith, D. M. Carbonaceous Particle Hydration. *Atmos. Environ.* **1999**, *33* (17), 2679−2687.
(22) Chughtai, A. R.; Kim, J. M.; Smith, D. M. The Effect of Air/Fuel Ratio on Properties and Reactivity of Combustion Soots. *J. Atmos. Chem.* **2002**, *43* (1), 21−43.
(23) Nguyen, T. H.; Sabbah, I.; Ball, W. P. Immobilization of Soot Particles in a Silica Matrix: A Sorbent-Carrier System for Studying Organic Chemical Sorption. *Environ. Sci. Technol.* **2005**, *39*, 6527−6534.
(24) Nguyen, T. H.; Brown, R. A.; Ball, W. P. An Evaluation of Thermal Resistance as a Measure of Black Carbon Content in Diesel Soot, Wood Char, and Sediment. *Org. Geochem.* **2004**, *35* (3), 217−234.
(25) *Standard Test Methods for Carbon Black—Surface Area by Multipoint B. E. T. Nitrogen Adsorption*; ASTM D 4820-97; American Society for Testing and Materials: Conshohocken, PA, 1998.
(26) *Determining Free-Space Values for Asap Series Micropore Analyses*; Micromeritics Application No. 104, Norcross, GA, Sept 2003.
(27) Olivier, J. P. Improving the Models Used for Calculating the Size Distribution of Micropore Volume of Activated Carbons from Adsorption Data. *Carbon* **1998**, *36* (10), 1469−1472.
(28) Barrett, E. P.; Joyner, L. G.; Halenda, P. P. The Determination of Pore Volume and Area Distributions in Porous Substances. 1. Computations from Nitrogen Isotherms. *J. Am. Chem. Soc.* **1951**, *73* (1), 373−380.
(29) Brunauer, S.; Emmett, P. H.; Teller, E. Adsorption of Gases in Multimolecular Layers. *J. Am. Chem. Soc.* **1938**, *60*, 309−319.
(30) Ball, W. P.; Roberts, P. V. Long-Term Sorption of Halogenated Organic Chemicals. Part 1. Equilibrium. *Environ. Sci. Technol.* **1991**, *25*, (7), 1223−1237.
(31) Carmo, A. M.; Hundal, L. S.; Thompson, M. L. Sorption of Hydrophobic Organic Compounds by Soil Materials: Application of Unit Equivalent Freundlich Coefficients. *Environ. Sci. Technol.* **2000**, *34* (20), 4363−4369.
(32) Dubinin, M. M.; Astakhov, V. A. Development of Concepts of Volume Filling of Micropores in Adsorption of Gases and Vapors by Microporous Adsorbents. *Izv. Akad. Nauk SSSR, Ser. Khim.* **1971**, *1*, 5−11.
(33) Xia, G.; Ball, W. P. Adsorption−Partitioning Uptake of Nine Low-Polarity Organic Chemicals on a Natural Sorbent. *Environ. Sci. Technol.* **1999**, *33* (2), 262−269.
(34) Manes, M. In *Encyclopedia of Environmental Analysis and Remediation*; Meyers, R. A., Ed.; John Wiley: New York, 1998.
(35) Kleineidam, S.; Rada, H.; Schuth, C.; Grathwohl, P. Solubility-Normalized Combined Pore-Filling-Partitioning Sorption Isotherms for Organic Pollutants. *Environ. Sci. Technol.* **2002**, *36* (21), 4689−4697.
(36) Sing, K. S. W.; Everett, D. H.; Haul, R. A. W.; Moscou, L.; Pierotti, R. A.; Rouquerol, J.; Siemieniewska, T. Reporting Physisorption Data for Gas Solid Systems with Special Reference to the Determination of Surface-Area and Porosity (Recommendations 1984). *Pure Appl. Chem.* **1985**, *57* (4), 603−619.
(37) Khachikian, C. S.; Harmon, T. C. Effects of Nonvolatile Organic Contamination on the Surface Areas and Adsorption Energetics of Porous Media. *Langmuir* **2000**, *16* (25), 9819−9824.
(38) Paulsen, P. D.; Moore, B. C.; Cannon, F. S. Applicability of Adsorption Equations to Argon, Nitrogen and Volatile Organic Compound Adsorption onto Activated Carbon. *Carbon* **1999**, *37* (11), 1843−1853.
(39) Schwarzenbach, R. P.; Gschwend, P. M.; Imboden, D. M. *Environmental Organic Chemistry*, 2nd ed.; Wiley-Interscience: New York, 2002.
(40) Crittenden, J. C.; Sanongraj, S.; Bulloch, J. L.; Hand, D. W.; Rogers, T. N.; Speth, T. F.; Ulmer, F. Correlation of Aqueous-Phase Adsorption Isotherms. *Environ. Sci. Technol.* **1999**, *33* (17), 2926−2933.
(41) Karanfil, T.; Kilduff, J. E. Role of Granular Activated Carbon Surface Chemistry on the Adsorption of Organic Compounds. 1. Priority Pollutants. *Environ. Sci. Technol.* **1999**, *33* (18), 3217−3224.
(42) Apicella, B.; Ciajolo, A.; Barbella, R.; Tregrossi, A. Size Exclusion Chromatography of Particulate Produced in Fuel-Rich Combustion of Different Fuels. *Energy Fuels* **2003**, *17* (3), 565−570.
(43) Kile, D. E.; Wershaw, R. L.; Chiou, C. T. Correlation of Soil and Sediment Organic Matter Polarity to Aqueous Sorption of Nonionic Compounds. *Environ. Sci. Technol.* **1999**, *33* (12), 2053−2056.
(44) Peters, C. A.; Mukherji, S.; Weber, W. J. Unifac Modeling of Multicomponent Nonaqueous Phase Liquids Containing Polycyclic Aromatic Hydrocarbons. *Environ. Toxicol. Chem.* **1999**, *18* (3), 426−429.

Received for review October 24, 2005. Revised manuscript received February 3, 2006. Accepted February 6, 2006.

ES052121A